DNA Binding of A D-Lysine-Based Chiral PNA: Direction Control and Mismatch Recognition

Stefano Sforza,[a] Roberto Corradini,[a] Silvia Ghirardi,[a] Arnaldo Dossena,[a] and Rosangela Marchelli*[a]

Keywords: Chirality / Direction control / DNA recognition / Mismatch recognition / Peptide nucleic acids

Peptide nucleic acids (PNAs) are oligonucleotide analogues with a skeleton made up of *N*-(2-aminoethyl)glycine units; they bind to complementary DNA and RNA with high stability and specificity. In order to improve the binding specificity, solubility and uptake into cells, many modifications have been introduced, some concerning the introduction of stereogenic centres. With the aim of achieving a selective antiparallel binding with DNA, we report in this paper the synthesis and binding abilities of a chiral PNA decamer (H-GTAG***ATC***ACT-NH_2) bearing three D-Lys-based monomers (a "chiral box") in the middle of the strand. Indeed, the antiparallel PNA-DNA duplex showed a melting point of 43 °C (determined both by CD and UV spectroscopy), whereas the parallel PNA-DNA duplex failed to form, as shown by the absence of temperature dependence in the UV and CD spectra. Moreover, hybridization experiments carried out with antiparallel DNA strands bearing single mismatches showed that this PNA was excellent in discriminating between mismatched and matched targets. These results indicate that a high chiral constraint in the middle of a PNA sequence strongly affects the direction selectivity, i.e. the antiparallel/parallel preference in the DNA complexation. In particular, a "D-chiral box" favours a highly specific antiparallel DNA binding, thus allowing possible diagnostic applications for the screening of single-point mutations.

Introduction

Peptide nucleic acids (PNAs) are oligonucleotide analogues with a skeleton made up of *N*-(2-aminoethyl)glycine units; they bind to complementary DNA and RNA with high stability and specificity.[1−4] Because of their excellent performance, they have been used in many biological and biochemical applications requiring selective recognition of nucleic acid sequences.[5]

In order to improve the binding specificity, solubility and uptake into cells, the PNA backbone has been modified in many ways. One particular approach involves the introduction of stereogenic centres,[6−10] most commonly based on different chiral aminoethylamino acids, first introduced and studied by Nielsen and co-workers (Figure 1).[7]

Chiral PNAs were generally found to form slightly less stable PNA-DNA duplexes than their achiral analogues,[7] the effect being more pronounced for backbones containing amino acids with bulky apolar side chains (such as those derived from phenylalanine or leucine).[11] Negatively charged monomers (derived from aspartic and glutamic acid) were shown to destabilize PNA-DNA duplexes further, probably because of the repulsive interactions with the DNA negatively charged phosphate groups.[12] On the other hand, by introducing positively charged lysine-based monomers, it was possible to obtain more stable PNA-DNA duplexes. As far as the configuration of the chiral monomers is concerned, PNAs containing D-monomers (D-PNAs) bind to the complementary antiparallel DNA with greater stability than do the corresponding L-PNAs.[12] The observed enantioselectivity had previously been explained[13] in terms of preferential PNA helicity induced by the configuration of the stereogenic centre. In particular, the D-monomers were supposed to induce a preferred right-handedness and the L-monomers a preferred left-handedness in the PNA strand: as a consequence, DNA, which is right-handed, would bind preferentially with the right-handed D-PNAs. This interpretation was indirectly confirmed by circular dichroism studies of the complexes between cyanine dyes and PNA-PNA and PNA-DNA duplexes.[14]

Moreover, with D-Lys-PNAs, it was observed that it was also possible to affect the direction selectivity, i.e. the anti-

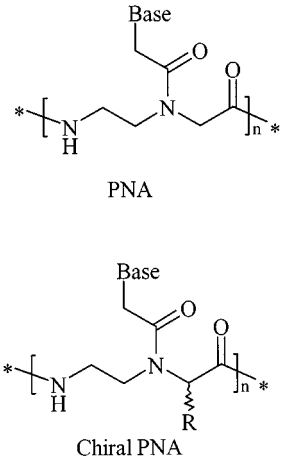

Figure 1. Achiral PNA (above) and chiral PNA (below). The latter is obtained by inserting a monomer based on a chiral amino acid

[a] Dipartimento di Chimica Organica e Industriale, Università di Parma
Area Parco delle Scienze 17/A, I-43100-Parma, Italy
Fax: (internat.) +39/0521-905472
E-Mail: marchell@ipruniv.cce.unipr.it

  1434−193X/00/0816−2905 $ 17.50+.50/0

parallel/parallel preference in the complexation of DNA. Indeed, D-Lys-containing PNAs showed an increased preference for the antiparallel mode of complexation, whereas the L-Lys-PNAs slightly improved the stability of the parallel binding.[13] Improved mismatch recognition was also reported for D-Lys-containing PNAs.[12]

Thus, it appears that the insertion of stereogenic centres derived from positively charged D-amino acids in suitable positions in the PNA strand can lead to more specific binding with complementary DNA, both in terms of complexation direction and of mismatch recognition. It has also been noted that the stereogenic centre was more efficient in affecting selectivity when it was positioned in the middle of the PNA strand.[13]

Therefore, it appears from the literature data that improvements in the specificity of DNA recognition by PNAs can be achieved by using chiral monomers with D-configuration, positive charge and a position in the middle of the PNA strand.

Consequently, in order to achieve a specific recognition of complementary antiparallel DNA, we decided to increase the chiral constraint in the middle of the PNA strand by inserting three adjacent chiral monomers based on D-lysine (a "chiral box"). The syntheses of three chiral PNA monomers ($T_{D\text{-}Lys}$, $C_{D\text{-}Lys}$, $A_{D\text{-}Lys}$) and of the PNA decamer H-GTAG($A_{D\text{-}Lys}$)($T_{D\text{-}Lys}$)($C_{D\text{-}Lys}$)ACT-NH_2 are reported here. The binding specificities (direction control and mismatch recognition) were studied by UV and CD spectroscopy, and comparisons made with the homologous achiral PNA.

Results and Discussion

PNA Synthesis

The Boc strategy was utilized for the PNA synthesis (Figure 2).

The following N_α-Boc-N_ε-(2-Cl-Cbz)-protected D-lysine chiral PNA monomers were synthesized first: Boc-$T_{D\text{-}Lys(2\text{-}Cl\text{-}Cbz)}$-OH **1a**, Boc-$C(Cbz)_{D\text{-}Lys(2\text{-}Cl\text{-}Cbz)}$-OH **1b** and Boc-$A(Cbz)_{D\text{-}Lys(2\text{-}Cl\text{-}Cbz)}$-OH **1c.** The thymine monomer **1a** was synthesized according to the literature,[12] while the cytosine and the adenine monomers **1b** and **1c** were synthesized here for the first time. Starting from N_α-Boc-N_ε-(2-Cl-Cbz)-D-Lys-OH **2**, (i) the free carboxyl group was protected as the allyl ester; (ii) the Boc group was then removed by treatment with *p*-toluenesulfonic acid; (iii) the free amino group was reductively aminated with *N*-Boc-aminoacetaldehyde, according to a procedure reported in the literature.[12] Then (iv) the D-aminoethyl-lysine allyl ester **3** was coupled with the appropriate carboxymethylnucleobase[15] to give the monomer esters **4a**, **4b** and **4c**; (v) the allyl ester was removed to yield the desired monomers **1a**, **1b** and **1c**. The monomers were purified by flash chromatography and characterized by spectroscopic methods. The optical purity was ascertained, using a chiral column (ChirasilVal), by the direct gas chromatographic method reported in the literature[16]. The *ee* was found to be always higher than 95%.

The monomers were then inserted into the middle of a PNA sequence already reported in the literature (the chiral monomers characterizing the "chiral box" are in bold characters and underlined): H-GTAG***ATC***ACT-NH_2 (**5**, Figure 3).[17]

The synthesis of PNA **5**, carried out on an MBHA resin[18] (final cleavage with trifluoromethanesulfonic acid), afforded the crude product in 95% yield. The product was purified by RP-HPLC and characterized by MALDI-TOF and API-ES mass spectrometry. The optical purity of the oligomer was ascertained by hydrolysis (6 N HCl) and analysis with the GC method previously reported.[16] The solid phase synthesis induced a small drop in optical purity (*ee* 90%). The achiral PNA of the same sequence (H-GTAGATCACT-NH_2, **6**) and the achiral complementary antiparallel PNA (H-AGTGATCTAC-NH_2, **7**) were also synthesized by the same procedure.

PNA-PNA Duplex Formation

The D-Lys-PNA **5** was hybridized with the complementary antiparallel achiral PNA **7** and the circular dichroism of the hybrid solution was measured. The circular dichroism spectrum showed the same shape as other D-lysine-containing PNA-PNA duplexes already reported in the literature, which, according to our assignment, were right-handed (Figure 4).[13]

As expected, the D-Lys-PNA **5** exhibited a preference for right-handedness in the PNA-PNA duplex and, the intensity of the CD signal being higher than that displayed by the PNA containing three scattered D-lysine monomers, we deduced that the mutual proximity of three D-Lysine side chains ("chiral box") considerably increases the preference for the right-handed helix.

The melting temperature of the D-Lys-PNA-PNA duplex was measured by UV and was found to be 56 °C, which is considerably lower than that measured for an achiral PNA-PNA duplex of the same sequence (65 °C).[13] This is a good indication that, together with an increased preference for right-handedness, the "chiral box" also induces a destabilization of the duplex, probably due to steric hindrance of the lysine side chains.

Antiparallel/Parallel Discrimination in DNA Recognition

Both chiral D-Lys PNA **5** and achiral PNA **6** were evaluated for their melting temperatures with the complementary antiparallel DNA (5′-dAGTGATCTAC-3′), as measured by UV. D-Lys-PNA **5** showed a melting temperature of 43 °C (Figure 5), significantly lower than that shown by the chiral PNA of the same sequence but with three separated chiral monomers (55 °C, ref. 13). This can be explained by considering the electrostatic interaction with the DNA strand as being the same in both cases − the number of charged groups in the two PNAs being the same − but with the steric hindrance due to the lysine side chains being

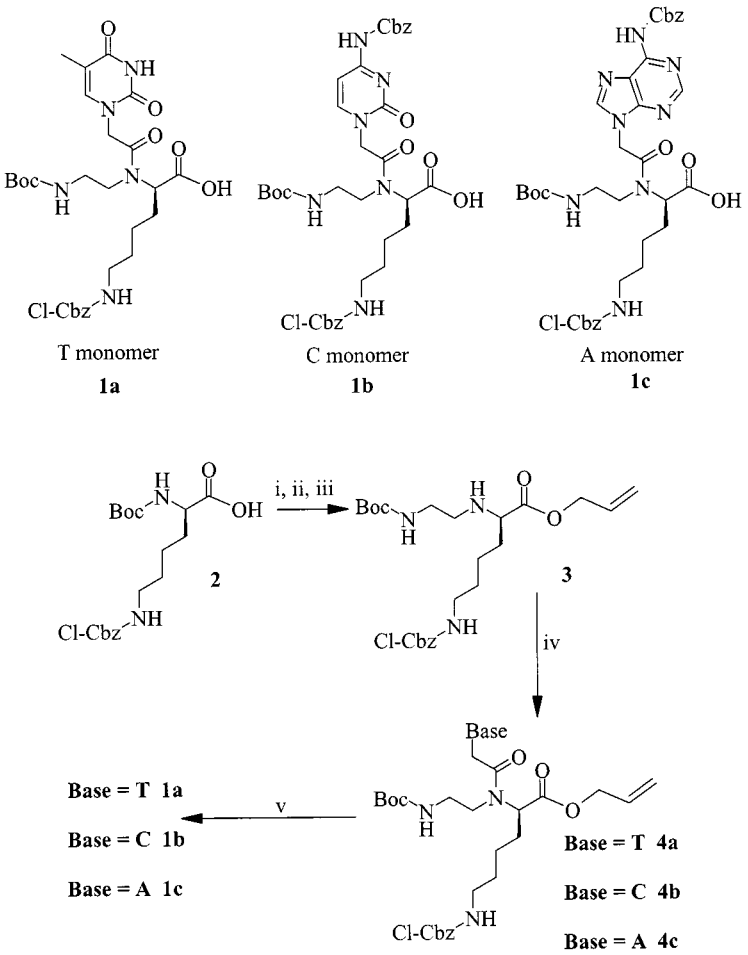

Figure 2. D-Lys-based PNA monomers containing thymine (**1a**), cytosine (**1b**) and adenine (**1c**) (above) and their synthesis (below). i) $CH_2{=}CHCH_2Br$, Cs_2CO_3, DMF, room temp., 70% yield; ii) *p*TSA, toluene, 100 °C, 97% yield; iii) Boc-Gly-H, $NaCNBH_3$, CH_3COOH, CH_3OH, 0 °C, 70% yield; iv) Base-CH_2COOH, DCC, DHBtOH, room temp. Yields: **4a** 72%, **4b** 90%, **4c** 41%. v) morpholine, $[Pd(PPh_3)_4]$, THF, room temp. Yields: **1a** 75%, **1b** 58%, **1c** 48%

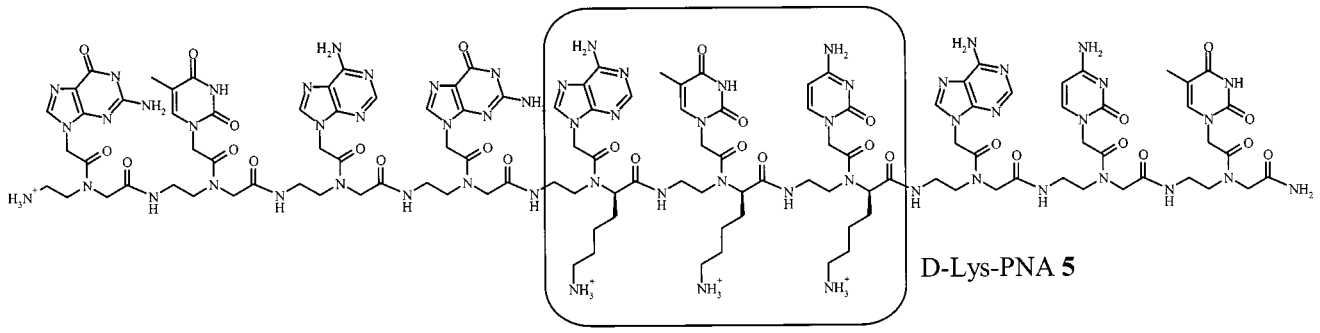

Figure 3. The D-Lys-PNA **5** (H-GTAG**ATC**ACT-NH_2) incorporating three chiral adjacent monomers (bold) in the middle of the strand

much greater for the D-Lys-PNA **5**, because of their mutual proximity. The melting temperature reported above is also lower than that displayed by the achiral PNA **6**-DNA duplex (50 °C, Figure 5), but still significantly higher than that of the corresponding DNA-DNA duplex (35 °C).[17] No "self-melt" transitions were observed between 15 and 70 °C for the D-Lys-PNA **5**.

In order to evaluate the direction selectivity, hybridization of D-Lys-PNA **5** with the complementary parallel DNA (5′-dCATCTAGTGA-3′) was attempted. In fact, the UV absorption at 260 nm between 15 and 70 °C was identical to that of the complementary DNA alone, showing no temperature dependence and thus indicating that the D-Lys-PNA **5** did not form a stable duplex (Figure 6) . In contrast, the achiral PNA **6** hybridized with the same target, exhibited a melting temperature of 41 °C, as already reported (Figure 6).[17]

Thus, from the UV data, it may be concluded that the D-Lys-PNA **5** described here exhibits a strong antiparallel/parallel selectivity in DNA binding.

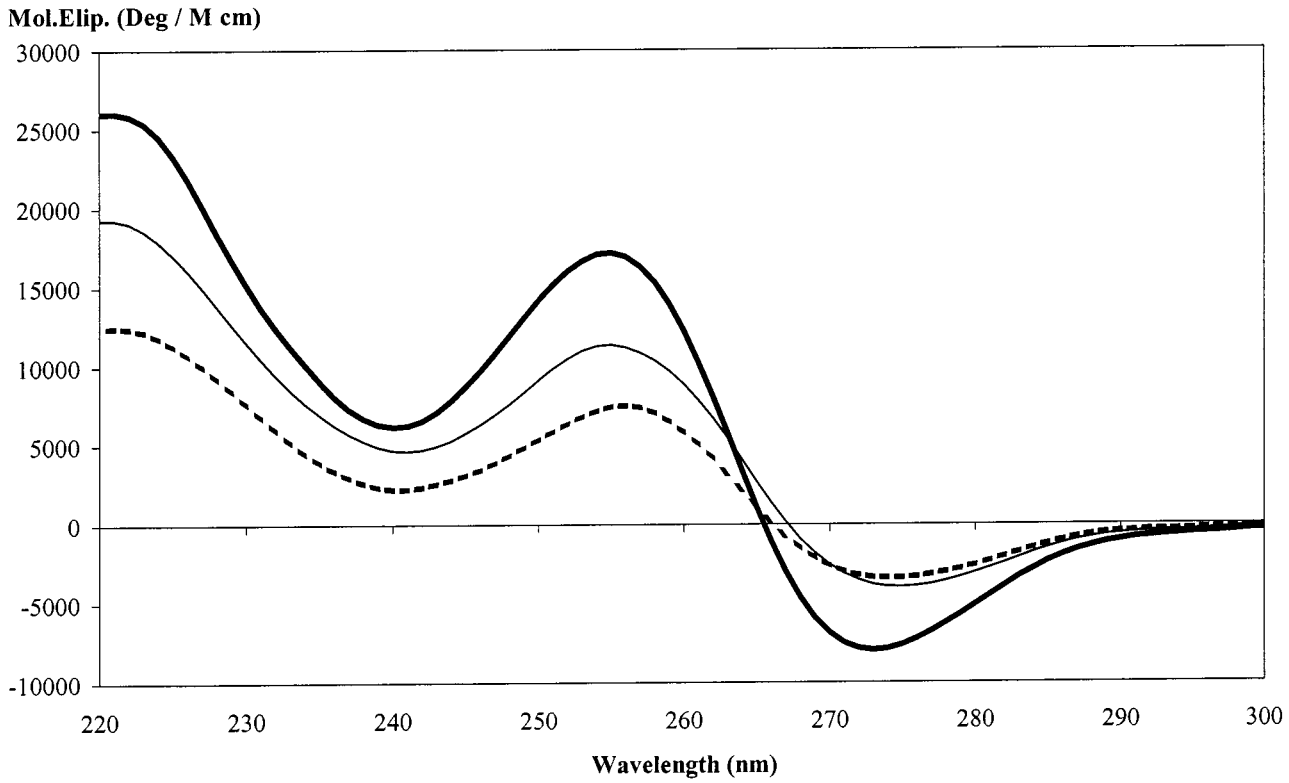

Figure 4. CD spectra of PNA-PNA duplexes formed by an achiral PNA (H-AGTGATCTAC-NH_2) and complementary chiral PNAs and incorporating D-Lys monomers in different positions: H-GTAGA***T***CACT-NH_2 (dotted line, one chiral monomer in the middle, from ref. [13]), H-G***T***AGA***T***CAC***T***-NH_2 (thin line, three scattered chiral monomers, from ref. [13]), H-GTAG***ATC***ACT-NH_2 (thick line, D-Lys-PNA **5**)

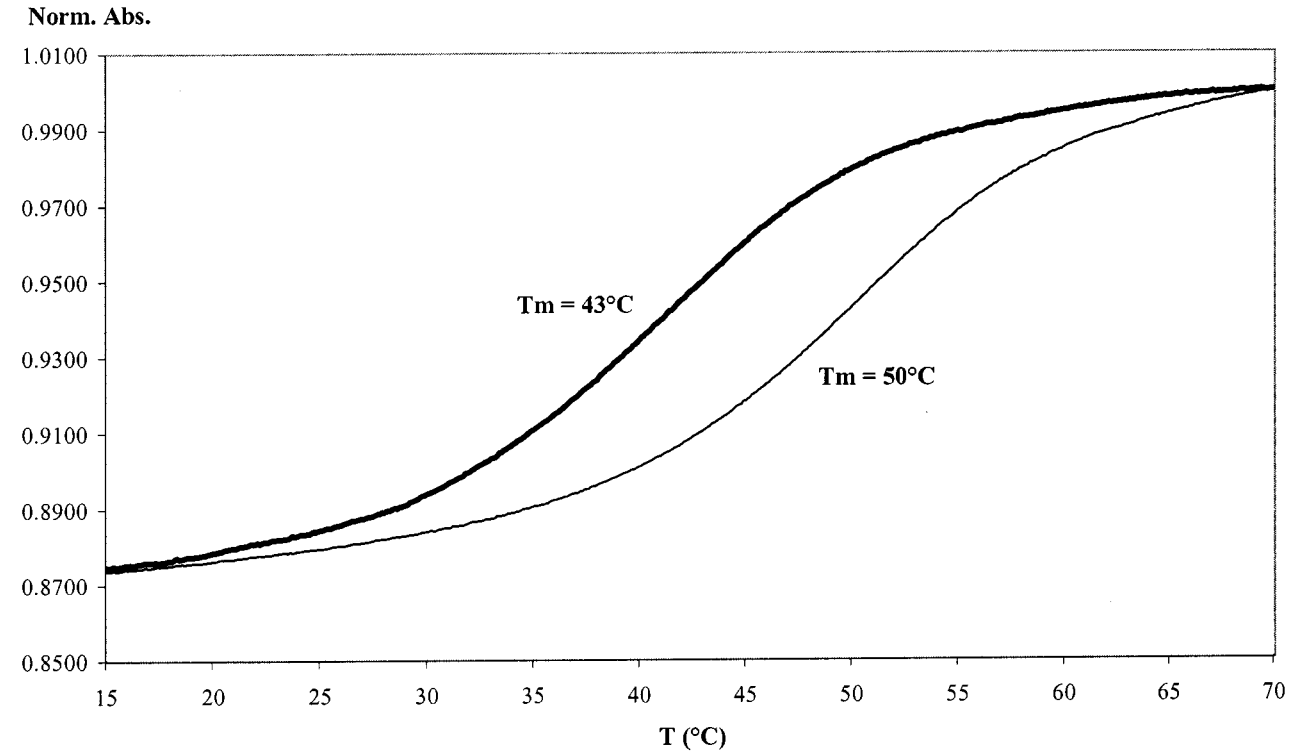

Figure 5. UV melting curves of the hybrid solutions formed by the D-Lys-PNA **5** (thick line) and by the analogous achiral PNA **6** (thin line) with the complementary antiparallel DNA

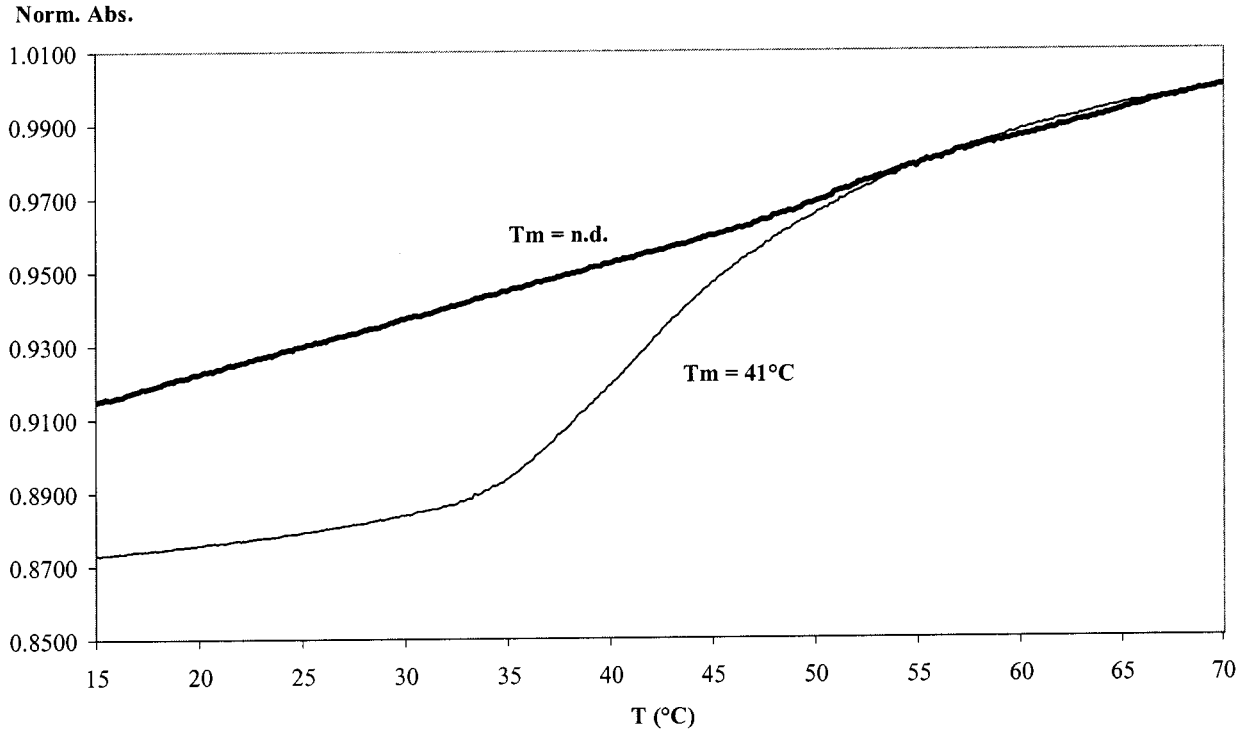

Figure 6. UV melting curves of the hybrid solutions formed by the D-Lys-PNA **5** (thick line) and by the analogous achiral PNA **6** (thin line) with the complementary parallel DNA

The antiparallel and the parallel PNA-DNA hybrid solutions were also analyzed by circular dichroism. The D-Lys-PNA **5** in the presence of the complementary antiparallel DNA showed a CD spectrum typical of an antiparallel PNA-DNA duplex,[13] whereas in the presence of the complementary parallel DNA it gave an undefined and much weaker CD spectrum (Figure 7).

Both solutions were heated in order to obtain CD melting curves (Figure 8). Again, the melting temperature of the antiparallel D-Lys-PNA **5**-DNA duplex was in good agreement with the value measured by UV (44 °C), whereas no temperature dependence was observed with the parallel DNA, thus confirming the direction selectivity in DNA binding.

A tentative hypothesis to explain the observed direction control may be as follows. The presence in the middle of the PNA strand of three chiral centres of D-configuration induces greater rigidity in the structure of the preferred right-handed helix, as clearly shown by the CD of the PNA-PNA duplex. Thus, the stability of the PNA-DNA duplex is favoured in entropic terms, but disfavoured by the steric hindrance of the lysine side chains, which proscribes perfect base-pairing. However, the affinity for the complementary antiparallel DNA is still remarkable, precisely on account of its compatible configuration and also of the positive charges on the lysine side chains, which give electrostatic interactions with the phosphate groups of DNA. On the other hand, when other destabilizing factors are present in the PNA-DNA duplex, such as with a parallel DNA target, the formation of the duplex becomes completely inhibited. Thus, the specificity of recognition becomes extremely high.

Mismatch Discrimination

The ability of the D-Lys-PNA **5** to discriminate mismatches in the target complementary antiparallel DNA was also assessed. Nine mismatched DNA targets were chosen: three with the mismatched base in position 4 (5′-AGT***X***ATCTAC-3′, with X = A, C, T), three with the mismatched base in position 5 (5′-AGTG***X***TCTAC-3′, with X = G, C, T) and three with the mismatched base in position 6 (5′-AGTGA***X***CTAC-3′, with X = G, C, A). The melting temperatures were measured by UV and by CD. The results are reported in Table 1.

The loss of stability caused by only one mismatched base is very remarkable, especially when the mismatch is sited in the middle of the "chiral box" (position 5), leading to unstable duplexes even at room temperature. When the corresponding mismatch is located in either side position (position 4 or 6), the destabilization is less pronounced.

In Table 2, the mismatch recognition of the D-Lys-PNA **5** is compared with the mismatch recognition of the achiral PNA **6** and with those of different PNAs, of the same sequence, already reported in the literature: one with a lysine connected to the C-terminus and two with three separated lysine monomers. The mismatched DNA target has the nucleobase guanine in place of adenine in position 5 of the DNA strand: 5′-AGTG***G***TCTAC-3′.

It may be deduced that the presence of chiral centre(s) in the PNA strand, deriving either from an amino acid connected to the C-terminus or from chiral monomers, results in good mismatch recognition. Very good results are obtained with the insertion of three chiral monomers of D-

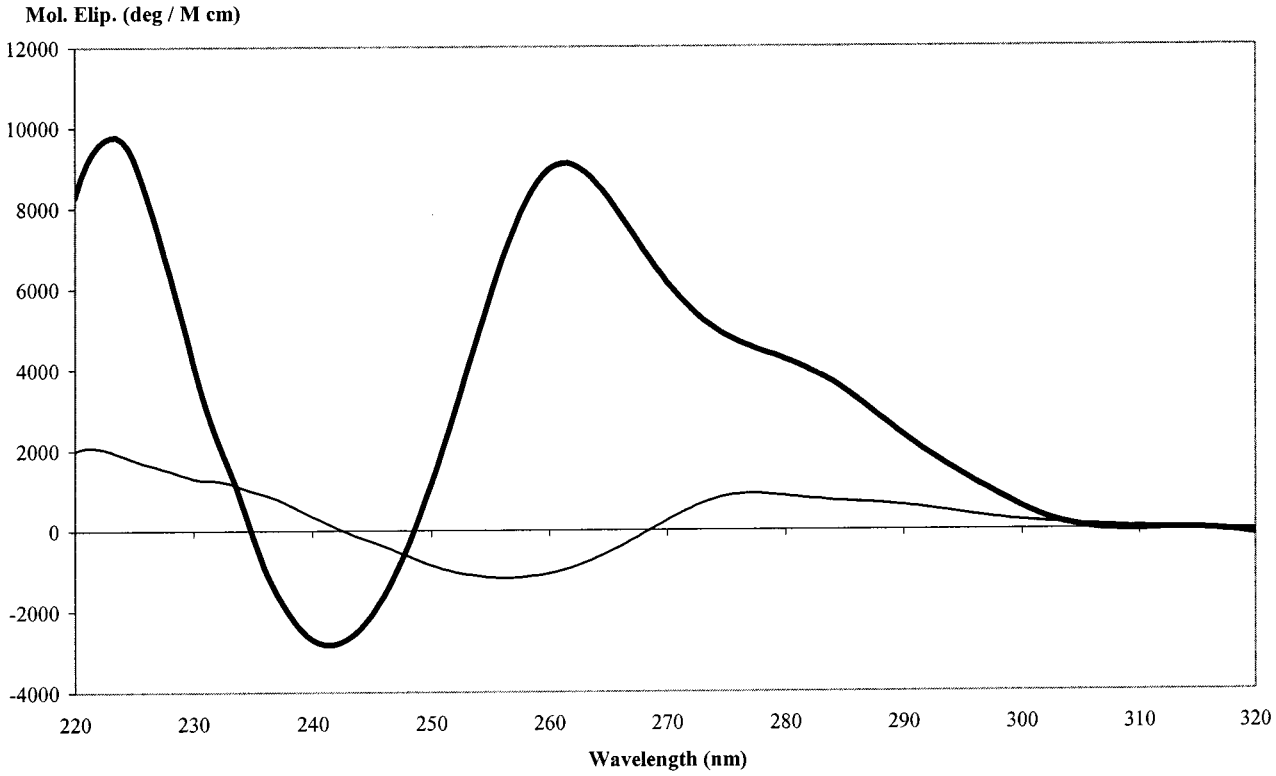

Figure 7. CD spectra of the hybrid solutions formed by the D-Lys-PNA **5** with the complementary antiparallel (thick lines) and parallel (thin lines) DNA

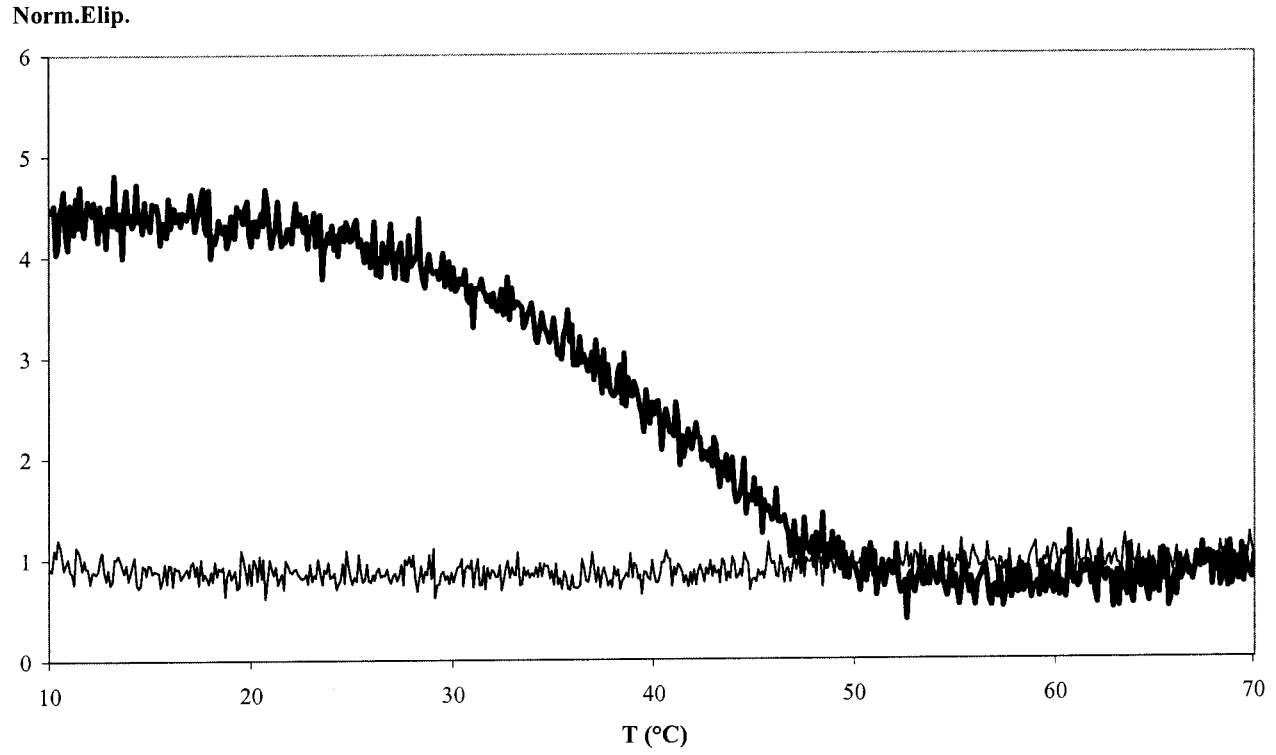

Figure 8. CD melting curves of the hybrid solutions formed by the D-Lys-PNA **5** with the complementary antiparallel (thick lines) and parallel (thin lines) DNA

Table 1. Melting temperatures of hybrid solutions formed by D-Lys-PNA **5** (H-GTAG**ATC**ACT-NH_2) with the complementary antiparallel mismatched and matched DNA targets

DNA-Base X	Position 4 5′-AGT***X***A**T**CTAC-3′ [a] T_m (°C)	Position 5 5′-AGT**G*X*T**CTAC-3′ [a] T_m (°C)	Position 6 5′-AGT**GA*X***CTAC-3′ [a] T_m (°C)
T	31	21	43 (full match)
A	28	43 (full match)	22
G	43 (full match)	–[b]	26
C	21	–[b]	23

[a] The DNA bases corresponding to the chiral monomers in the PNA are in bold characters – [b] No temperature dependence in the UV curve was observed between 15 and 70 °C

Table 2. Melting temperatures of different homologous PNAs with the matched and singly-mismatched DNA target. Matched sequence: 5′-AGTGATCTAC-3′; mismatched sequence: 5′-AGTG***G***TCTAC-3′

PNA	T_m (°C) matched	T_m (°C) mismatched	ΔT_m (°C)
H-GTAGATCACT-NH_2, **6**	50	40	–10
H-GTAGATCACT-($_L$-Lys)-NH_2	52[12]	37[12]	–15[12]
H-G($T_{L\text{-}Lys}$)AGA($T_{L\text{-}Lys}$)CAC($T_{L\text{-}Lys}$)-(^{l}-Lys)-NH_2	49[12]	35[12]	–14[12]
H-G($T_{D\text{-}Lys}$)AGA($T_{D\text{-}Lys}$)CAC($T_{D\text{-}Lys}$)-(^{l}-Lys)-NH_2	55[12]	36[12]	–19[12]
H-GTAG($A_{D\text{-}Lys}$)($T_{D\text{-}Lys}$)($C_{D\text{-}Lys}$)ACT-NH_2, **5**	43	–[a]	–[a]

[a] No temperature dependence in the UV curve was observed between 15 and 70 °C

configuration (ΔT_m = –19 °C). When the three D-monomers are inserted in the middle of the strand ("chiral box"), as in D-Lys-PNA **5**, the effect is magnified and the PNA perfectly discriminates the mismatched DNA target.

Thus, the presence of a chiral constraint ("chiral box") in the middle of the PNA strand substantially improves the discrimination between matched and mismatched DNAs, probably because of the same factors involved in the direction control.

Conclusions

The chiral D-Lys-PNA **5**, based on three adjacent D-lysine monomers ("chiral box") in the middle of the strand, binds to DNA in exclusively antiparallel fashion, showing no affinity for the parallel DNA target. This is in marked contrast to achiral PNA. Thus, this type of PNA overcomes the lack of binding selectivity in the direction control. Moreover, the same PNA also displayed very good single-point mismatch recognition.

Both effects seem to arise from a delicate balance between stabilizing and destabilizing factors. The correct D-configuration (entropy effect) and the presence of positive charges (enthalpy effect) favour the duplex formation, whereas steric effects induce destabilization. Hence, in the antiparallel matched PNA-DNA duplex, good binding still occurs, whereas when new destabilizing factors intervene (parallel or mismatched duplexes), it is prevented.

Further studies will be needed in order to elucidate whether this effect can be generalized to other PNA sequences incorporating chiral constraints in their backbones and to understand the structural requirements for the binding preference.

Finally, these effects, if confirmed for other sequences, could be exploited for the synthesis of new PNAs capable of acting in diagnostics as more specific tools for the detection of point mutations and in therapeutics as potentially more specific antisense and/or antigene drugs.

Experimental Section

General: Boc: *tert*-butoxycarbonyl; Cbz: carbobenzoxycarbonyl; DCC: *N*,*N*′-dicyclohexylcarbodiimide; DCU: *N*,*N*′-dicyclohexylurea; DMF: *N*,*N*-dimethylformamide; DMSO: *N*,*N*-dimethyl sulfoxide; DHBtOH: 3-hydroxy-1,2,3-benzotriazin-4(3*H*)-one; HBTU: *O*-(1*H*-benzotriazol-1-yl)-*N*,*N*,*N*′,*N*′-tetramethyluronium hexafluorophosphate; Lys: lysine; TFMSA: trifluoromethanesulfonic acid; TFA: trifluoroacetic acid.

The abbreviations used for the nucleobases (T, C, A, G) indicate different chemical structures in PNA and DNA oligomers; in the former case the nucleobase is connected to a pseudopeptide backbone, in the latter to a sugar-phosphate one. The sequences are given in the N to C direction in the case of PNA, and in the 5′ to 3′ direction in the case of DNA.

Synthesis of the Chiral Monomers (1a, 1b, 1c). – Boc-$T_{D\text{-}Lys(2\text{-}Cl\text{-}Cbz)}$-OH monomer (1a): The Boc-$T_{D\text{-}Lys(2\text{-}Cl\text{-}Cbz)}$-OH monomer was synthesized according to the literature procedure.[12] *Ee* (chiral GC-MS/MS according to the method reported in the literature):[16] 95%.

***N*′-Boc-N_ε-(2-Cl-Cbz)-aminoethyl-D-lysine-*O*-All (3):** The protected backbone was synthesized according to the literature procedure.[12]

Carboxymethylnucleobases: The carboxymethylthymine and the Cbz-protected carboxymethyladenine and carboxymethylcytosine were synthesized as reported in the literature.[15]

Boc-C(Cbz)$_{D\text{-}Lys(2\text{-}Cl\text{-}Cbz)}$-OAll (4b) and Boc-A(Cbz)$_{D\text{-}Lys(2\text{-}Cl\text{-}Cbz)}$-OAll (4c): The appropriate Cbz-protected nucleobase-substituted

acetic acid (0.8 mmol, either cytosine or adenine) was dissolved in DMF (8 mL) at 0 °C, together with DHBtOH (0.8 mmol) and DCC (0.8 mmol). The solution was stirred for 1.5 h at 0 °C, then for 45 min. at room temperature. The DCU was then filtered and the protected lysine backbone (0.4 mmol) was added to the solution. The solution was stirred overnight and the DMF was then evaporated. The residue was taken up in dichloromethane and washed with saturated potassium hydrogen sulfate (2 times) and saturated sodium hydrogen carbonate (2 times). The organic solution was dried over magnesium sulfate and filtered, solvent was removed and the residue was purified by flash chromatography (dichloromethane/methanol 98:2). The adenine monomer ester 4c required a further purification by flash chromatography (ethyl acetate/methanol 98:2).

Boc-C(Cbz)$_{D\text{-}Lys(2\text{-}Cl\text{-}Cbz)}$-OAll (4b): Yield 90%. − ^{1}H NMR (300 MHz, [D$_6$]DMSO, major rotamer only): δ = 1.38 (s, 9 H, CH$_3$ Boc), 1.2−1.5 (m, 6 H, −CH$_2$−CH$_2$−CH$_2$- Lys side chain), 2.8−3.2 (m, 6 H, −CH$_2$−CH$_2$- aminoethyl group + −CH$_2$−N Lys side chain), 4.37 (s br, 1 H, C$_\alpha$-H), 4.52 (d, ^3J = 4.8 Hz, 2 H, CH$_2$ allyl), 4.81 (s, 2 H, OC−CH$_2$−cytosine), 5.08 (s, 2 H, CH$_2$ Cl-*Z*), 5.1−5.2 (m, 1 H, CH−H(trans) allyl), 5.18 (s, 2 H, CH$_2$ *Z*-cytosine), 5.29 (dd, ^3J = 17.3 Hz, ^2J = 1.6 Hz, 1 H, CH−H(*cis*) allyl), 5.8−6.0 (m, 1 H, C−H allyl), 6.91 (s br, 1 H, N−H Boc), 7.02 (d, ^3J = 7.3 Hz, 1 H, C−H cytosine), 7.3−7.5 (m, 10 H, aromatic C−H *Z*-cytosine + 2-Cl-*Z*-lysine), 7.94 (d, ^3J = 7.3 Hz, 1 H, C−H cytosine), 10.79 (s, 1 H, N−H *Z*-cytosine). − ^{13}C NMR (300 MHz, [D$_6$]DMSO): δ = 22.9, 24.3, 28.0, 29.0, 33.2, 47.4, 49.7, 54.7, 59.1, 62.4, 64.9, 66.3, 77.9, 93.7, 117.6, 127.1, 127.7, 128.0, 128.3, 129.1, 129.5, 132.3, 134.5, 135.8, 150.7, 154.8, 155.6, 163.1, 167.2, 170.1. − FT-IR (liquid film): $\tilde{\nu}$ = 3331 (s), 2935 (m), 1700 (m), 1664 (m), 1213 (m) cm^{-1}. − ESI-MS: calcd. *m*/*z* 783.3 (MH$^+$); found *m*/*z* 784.

Boc-A(Cbz)$_{D\text{-}Lys(2\text{-}Cl\text{-}Cbz)}$-OAll (4c): Yield: 50%. − ^{1}H NMR (300 MHz, [D$_6$]DMSO, major rotamer only): δ = 1.39 (s, 9 H, CH$_3$ Boc), 1.3−2.0 (m, 6 H, −CH$_2$−CH$_2$−CH$_2$- Lys side chain), 2.9−3.5 (m, 6 H, −CH$_2$−CH$_2$- aminoethyl group + −CH$_2$−N Lys side chain), 4.31 (s br, 1 H, C$_\alpha$−H), 4.50 (d, ^3J = 5.1 Hz, 2 H, CH$_2$ allyl), 5.09 (s, 2 H, CH$_2$ Cl-*Z*), 5.15 (dd, ^3J = 10.5, ^2J = 1.3 Hz, 2 H, CH−H(*trans*) allyl), 5.22 (s, 2 H, CH$_2$ *Z*-adenine), 5.3−5.4 (m, 3 H, OC−CH$_2$−adenine + CH−H(cis) allyl), 5.8−5.9 (m, 1 H, C−H allyl), 6.94 (s br, 1 H, N−H Boc),), 7.3−7.5 (m, 10 H, aromatic C−H *Z*-adenine + 2-Cl-*Z*-lysine), 8.33 (s, 1 H, aromatic C−H adenine), 8.59 (s, 1 H, aromatic C−H adenine), 10.6−10.7 (s br, 1 H, N−H *Z*-adenine). − ^{13}C NMR (300 MHz, [D$_6$]DMSO): δ = 23.1, 28.1, 29.1, 44.1, 52.5, 54.8, 59.6, 62.5, 64.9, 66.2, 78.0, 117.6, 123.0, 127.2, 127.8, 127.9, 128.4, 129.2, 129.6, 132.3, 134.6, 136.3, 144.6, 149.3, 149.5, 151.7, 152.1, 155.8, 166.6, 170.0. − FT-IR (liquid film): $\tilde{\nu}$ = 3347 (m), 2938 (m), 1708 (s), 1589 (s), 1215 (s), 1161 (s) cm^{-1}. ESI-MS: calcd. *m*/*z* 807.3 (MH$^+$); found *m*/*z* 808.

Boc-C(Cbz)$_{D\text{-}Lys(2\text{-}Cl\text{-}Cbz)}$-OH (1b) and Boc-A(Cbz)$_{D\text{-}Lys(2\text{-}Cl\text{-}Cbz)}$-OH (1c): The appropriate (Cbz-nucleobase)-Boc-protected monomer allyl ester (0.5 mmol, either with cytosine or with adenine) was dissolved in THF (8 mL), together with morpholine (5 mmol) and [Pd(PPh$_3$)$_4$] (0.05 mmol). After 10 minutes, additional [Pd(PPh$_3$)$_4$] (0.05 mmol) was added and the reaction was stirred for 30 minutes. The mixture was then evaporated and the residue was recovered in ethyl acetate and washed with saturated potassium hydrogen sulfate (2 times) The aqueous solution was then washed several times with ethyl acetate. The combined organic phases were dried over magnesium sulfate and filtered, and solvent was evaporated under vacuum. The residue was purified by flash chromatography (dichloromethane/methanol, gradient elution from CH_2Cl_2:MeOH 95:5 to 100% MeOH). The monomers were obtained as white solids by precipitation from THF/hexane.

Boc-C(Cbz)$_{D\text{-}Lys(2\text{-}Cl\text{-}Cbz)}$-OH (1b): Yield: 58%. − ^{1}H NMR (300 MHz, [D$_6$]DMSO, major rotamer only): δ = 1.35 (s, 9 H, CH$_3$ Boc), 1.0−1.5 (m, 6 H, −CH$_2$−CH$_2$−CH$_2$- Lys side chain), 2.9−3.3 (m, 6 H, −CH$_2$−CH$_2$- aminoethyl group + −CH$_2$−N Lys side chain), 3.76 (s br, 1 H, C$_\alpha$−H), 4.68 (s, 2 H, OC−CH$_2$−cytosine), 5.08 (s, 2 H, CH$_2$ Cl-*Z*), 5.19 (s, 2 H, CH$_2$ *Z*-cytosine), 6.97 (d, ^3J = 7.1 Hz, 1 H, C−H cytosine), 7.14 (s br, 1 H, N−H Boc), 7.3−7.5 (m, 10 H, aromatic C−H *Z*-cytosine + 2-Cl-*Z*-lysine), 7.86 (d, ^3J = 7.3 Hz, 1 H, C−H cytosine), 10.77 (s br, 1 H, N−H *Z*-cytosine). − ^{13}C NMR (300 MHz, [D$_6$]DMSO): δ = 23.1, 24.4, 25.3, 28.1, 29.1, 47.5, 58.9, 62.5, 66.4, 67.4, 78.0, 93.8, 127.3, 127.9, 128.1, 128.4, 128.6, 128.8, 129.2, 129.6, 132.2, 134.6, 135.9, 150.9, 153.2, 154.9, 155.7, 163.1, 167.2. FT-IR (liquid film): $\tilde{\nu}$ = 3325 (w), 2928 (m), 1700 (m), 1663 (m), 1509 (m), 1216 (m) cm^{-1}. − ESI-MS: calcd. 743.3 (MH$^+$); found 744. *Ee* (chiral GC-MS according to the method reported in the literature):[16] 95%.

Boc-A(Cbz)$_{D\text{-}Lys(2\text{-}Cl\text{-}Cbz)}$-OH (1c): Yield: 48%. − ^{1}H NMR (300 MHz, [D$_6$]DMSO, major rotamer only): δ = 1.39 (s, 9 H, CH$_3$ Boc), 1.1−1.5 (m, 6 H, −CH$_2$−CH$_2$−CH$_2$- Lys side chain), 2.9−3.2 (m, 6 H, −CH$_2$−CH$_2$- aminoethyl group + −CH$_2$−N Lys side chain), 4.22 (s br, 1 H, C$_\alpha$−H), 5.09 (s, 2 H, CH$_2$ Cl-*Z*), 5.22 (s, 2 H, CH$_2$ *Z*-adenine), 5.32 (s, 2 H, OC−CH$_2$−adenine), 6.99 (s br, 1 H, N−H Boc),), 7.3−7.5 (m, 10 H, aromatic C−H *Z*-adenine + 2-Cl-*Z*-lysine), 8.34 (s, 1 H, aromatic C−H adenine), 8.58 (s, 1 H, aromatic C−H adenine), 10.60 (s br, 1 H, N−H *Z*-adenine). − ^{13}C NMR (300 MHz, [D$_6$]DMSO): δ = 24.1, 28.2, 29.2, 44.3, 44.7, 54.9, 62.5, 66.2, 77.0, 122.5, 127.3, 127.8, 128.0, 128.4, 129.2, 129.6, 134.6, 136.3, 145.5, 149.2, 151.4, 152.2, 155.8, 167.3, 173.6. − FT-IR (liquid film): $\tilde{\nu}$ = 3338 (m), 2927 (m), 1706 (m), 1617 (s), 1216 (s), 1162 (s) cm^{-1}. − ESI-MS: calcd. 767.3 (MH$^+$); found 768. *Ee* (chiral GC-MS according to the method reported in the literature):[16] 97%.

PNA Synthesis: The PNA syntheses were performed following the standard procedure on a (4-methylbenzhydryl)-amine resin (Novabiochem), using HBTU/diethylcyclohexylamine as coupling reagent in DMF/pyridine.[12,13,18] The syntheses were performed on a 6 μmol scale. The free PNAs were cleaved from the resin using a TFMSA/TFA mixture (typical yield of the crude product: 80−90%). HPLC purification was carried out on a C$_{18}$ column (eluent: water-acetonitrile mixtures with 0.1% TFA; gradient: from 100% water to 100% acetonitrile in 25 minutes, flow 1 mL/min).

H-GTAG(A-D-Lys)(T-D-Lys)(C-D-Lys)ACT-NH$_2$ (D-Lys-PNA 5): MALDI: calcd. *m*/*z* 2940 (MH$^+$); found *m*/*z* 2939; ESI: calcd. *m*/*z* 980.7 (MH$_3^{3+}$); found *m*/*z* 981. *Ee* (chiral GC-MS according to the method reported in the literature):[16] 90%.

H-GTAGATCACT-NH$_2$ (Achiral PNA 6): ESI: calcd. *m*/*z* 910.2 (MH$_3^{3+}$); found *m*/*z* 910.

H-AGTGATCTAC-NH$_2$ (Achiral PNA 7): MALDI: calcd. *m*/*z* 2728 (MH$^+$); found *m*/*z* 2730.

Hybridization Experiments: The DNA sequences used in the hybridization experiments were purchased from Genset (France). All hybrid samples reported were first incubated at 90 °C for 5 minutes, then slowly cooled at room temperature. The total strand concentration for each sample was calculated using the following ε_{260} (mM^{-1} cm^{-1}) for the four bases: T 8.8, C 7.3, A 10.4, G 11.7. All

hybridization experiments were carried out in a 10 mM phosphate buffer, 100 mM NaCl, 0.1 mM EDTA, pH = 7. Melting curves were recorded by heating the samples (1 °C/min) and following the CD or UV signal variation at 260 nm. Melting temperatures were taken as the maximum of the first derivative of the melting curves. The UV data were recorded on a Kontron Uvikon 922 spectophotometer. The CD data were recorded on a Jasco J715 spectropolarimeter.

Acknowledgments

This work was supported by CNR (Consiglio Nazionale delle Ricerche-Target Project on Biotechnology) and by MURST (Ministero dell'Università e della Ricerca Scientifica e Tecnologica – "Applications of PNAs, ribozymes and peptides for the study of gene expression and development of new diagnostic and therapeutic strategies").

[1] P. E. Nielsen, M. Egholm, R. H. Berg, O. Buchardt, *Science* **1991**, *254*, 1497−1500.
[2] M. Egholm, O. Buchardt, P. E. Nielsen, R. H. Berg, *J. Am. Chem. Soc.* **1992**, 114, 1895−1897.
[3] B. Hyrup, P. E. Nielsen, *Bioorg. Med. Chem.* **1996**, *4*, 5−23.
[4] M. Egholm, O. Buchardt, L. Christensen, C. Behrens, S. M. Freier, D. A. Driver, R. H. Berg, S. K. Kim, B. Norden, P. E. Nielsen, *Nature* **1993**, *365*, 566−568.
[5] E. Uhlmann, A. Peyman, G. Breipohl, D. W. Will, *Angew. Chem. Int. Ed*. **1998**, *37*, 2796−2893.
[6] L. Kosynkina, W. Wang, T. C. Liang, *Tetrahedron Lett.* **1994**, *35*, 5173−5176.
[7] K. L. Duheolm, K. H. Petersen, D. K. Jensen, M. Egholm, P. E. Nielsen, O. Buchardt, *Bioorg. Med. Chem. Lett.* **1994**, *4*, 1077−1080.
[8] K. H. Petersen, O. Buchardt, P. E. Nielsen, *Bioorg. Med. Chem. Lett.* **1996**, *6*, 793−796.
[9] B. P. Gangamani, V. A. Kumar, *Tetrahedron* **1996**, *52*, 15017−15030.
[10] P. Lagriffoule, P. Wittung, M. Eriksson, K. K. Jensen, B. Norden, O. Buchardt, P. E. Nielsen, *Chem. Eur. J.* **1997**, *3*, 912−919.
[11] A. Puschl, S. Sforza, G. Haaima, O. Dahl, P. E. Nielsen, *Tetrahedron Lett.* **1998**, *39*, 4707−4710.
[12] G. Haaima, A. Lohse, O. Buchardt, P. E. Nielsen, *Angew. Chem. Int. Ed. Engl.* **1996**, *35*, 1939−1941.
[13] S. Sforza, G. Haaima, R. Marchelli, P. E. Nielsen, *Eur. J. Org. Chem.* **1999**, 197−204.
[14] J. O. Smith, D. A. Olson, B. A. Armitage, *J. Am. Chem. Soc.* **1999**, *121*, 2686−2695.
[15] S. A. Thomson, J. A. Josey, R. Cadilla, M. D. Gaul, C. F. Hassman, M. J. Luzzio, A. J. Pipe, K. L. Reed, D. J. Ricca, R. W. Wiethe, S. A. Noble, *Tetrahedron* **1995**, *51*, 6179−6194.
[16] R. Corradini, G. Di Silvestro, S. Sforza, G. Palla, A. Dossena, P. E. Nielsen, R. Marchelli, *Tetrahedron Asymm.* **1999**, *10*, 2063−2066.
[17] P. Wittung, P. E. Nielsen, O. Buchardt, M. Egholm, B. Norden, *Nature* **1994**, *368*, 561−563.
[18] L. Christensen, R. Fitzpatrick, B. Gildea, K. H. Petersen, H. F. Hansen, T. Koch, M. Egholm, O. Buchardt, P. E. Nielsen, J. Coull, R. H. Berg, *J. Peptide. Sci.* **1995**, *3*, 175−183.

Received January 12, 2000
[O00014]